JOURNAL OF MATERIALS SCIENCE 30 (1995) 2108–2114

Characterization of zinc phosphate coatings obtained from modified baths

U. B. NAIR, M. SUBBAIYAN
Department of Analytical Chemistry, University of Madras, Guindy Campus, Madras 600 025, India

Zinc phosphate coatings obtained from phosphating baths modified with long-chain flotation surfactants, were characterized by scanning electron microscopy, X-ray diffraction and X-ray photoelectron spectroscopy techniques. The results of these characterization studies were correlated to the mechanism proposed to explain the influence of these additives on the nature and quality of the phosphate coatings obtained in their presence, as well as to explain the behaviour of these coatings in aggressive environments. These studies indicate that the surfactant additives not only control the initial nucleation process but also participate during the subsequent stages of coating deposition, and regulate its growth.

1. Introduction

The modification of metal surfaces through the use of phosphate pretreatments is a well-known method of improving their corrosion resistance, workability and paint-base properties. Although these conversion coatings, in themselves, provide little or no structural strength or corrosion protection, they play a significant role in the elimination of costly service failures by controlling under-film corrosion when used in conjunction with other finishes [1, 2].

Conventional phosphating formulations often need to be modified, in order to suit the end use to which the coating is put. To suitably modify a phosphating formulation, it is essential to have a good understanding of the chemistry of the phosphating process and the complex phenomena involved in the nucleation and growth of phosphate crystals. This has led to the widespread use of electrochemical [3–5] and analytical techniques [6, 7] to characterize the features and properties of phosphate coatings.

Virtually every spectroscopic technique has been used to study the diverse characteristics of phosphate coatings, including their crystal size, crystal type and orientation, crystal density, microtopography, morphology and composition, as well as the steps involved in their nucleation and growth. Infrared spectroscopy (IR) has been used to determine the steps involved in phosphating and the phases formed in phosphate coatings [8]. Electron spin resonance spectroscopy (ESR) has been used to confirm the modified structure of hopeite formed on the surface of coated steel sheets [9]. X-ray fluorescence (XRF) has been used to investigate the chemical state of nickel in coatings obtained from modified zinc phosphating baths [9]. Rudolf and Hansen [10] have used electron probe microanalysis (EPMA) to determine the composition and porosity of phosphate coatings, while Nomura and Ujihara [11] have used conversion electron Mössbauer spectrometry (CEMS) and transmission Mössbauer spectrometry (TMS) to study the formation and thermal properties of manganese phosphate coatings. Laser Raman spectroscopy [12] has been used to study the structure of hopeite, while details on the changes in the structure of hopeite following the modification of zinc phosphating baths with manganese have been studied by X-ray absorption near-edge structure (XANES) and extended X-ray absorption fine structure (EXAFS) [13] techniques.

X-ray diffraction (XRD) technique has been used to determine the crystal type and crystal orientation of the major phases present in phosphate coatings [14]. Further, the relative proportions of the various phases can also be determined by this method, which can, in turn, be related to the coating stability, corrosion resistance, etc. [15]. The nature of the phosphated surface and its microtopography have been determined using scanning electron microscopy (SEM). Grain morphology, grain size, grain distribution, uniformity of the coating, etc., may also be determined using this method [4, 8, 10].

More recently, surface microanalytical techniques such as X-ray photoelectron spectroscopy (XPS) and Auger electron spectroscopy (AES), have emerged as powerful aids in assisting the study of the mechanisms of aqueous corrosion processes [16] and in providing valuable information on interfacial interactions that govern failures of polymeric finishes on pretreated metal surfaces [17]. In combination with depth profiling, these techniques have also been used to evaluate post-treatments on phosphated steels [18], interaction of polymeric additives on zinc phosphate coatings [19], changes in morphological and chemical properties of phosphate crystals obtained on different types of steel substrates [20], etc.

Our earlier studies on the evaluation of some structurally similar long-chain flotation surfactants as

0020–2461

additives in a calcium-modified cold zinc phosphating bath indicated that phosphate coatings of desirable properties [21, 22] were obtained in the presence of low concentrations of these additives. Significant differences in bath chemistry were also observed which were attributed to the differences in the functional groups present in these additives [21]. In the present study, phosphate coatings obtained from the formulated calcium–zinc cold phosphating bath containing 1-octadecanethiol (1-ODT) and its non-thio analogue (1-octadecanol (1-ODol)) were characterized with a view to obtaining information on the nature of their interactions with phosphate coatings. Besides the determination of chemical composition at various strata of the coatings through X-ray photoelectron spectroscopy, structural information was sought by performing X-ray diffraction and scanning electron microscopy, in order to correlate this information to the proposed mode of action of these additives in the formulated phosphating bath.

2. Experimental procedure

A cold phosphating bath of the following composition was used in the present study: zinc oxide $9\ g\,l^{-1}$, *o*-phosphoric acid $20\ ml\,l^{-1}$, calcium carbonate $1\ g\,l^{-1}$, and sodium nitrite $2\ g\,l^{-1}$. Immersion phosphating of hot-rolled mild steel panels (IS 1079) of $96\ cm^2$ surface area was carried out for 30 min at room temperature (27 °C) in a processing sequence which included degreasing, pickling and rinsing prior to phosphating. An optimum concentration of $50\ mg\,l^{-1}$ 1-ODol and $75\ mg\,l^{-1}$ 1-ODT, respectively [21], were added to the formulated bath and the coatings obtained from the modified baths and the reference bath (containing no additive) were evaluated for their physical properties and corrosion performance.

The coatings obtained from the reference and the additive-containing baths were characterized. The surface microtopology of the phosphate coatings was evaluated using a Cambridge Stereoscan 180 model scanning electron microscope operating at 32 kV, under a pressure of 10^{-7} torr. The crystallinity and phase constituents of these coatings were evaluated using a Reich Seifert (XRD 3000 P model) X-ray diffractometer, operating at 35 kV using a copper target and nickel filter. The X-ray diffractograms were recorded in a 2θ angle range of 5°–6°, at a scan rate of $1.8°\ min^{-1}$. The surface chemical composition of the phosphated panels was determined using a VG Scientific X-ray photoelectron spectrometer (model ESCALAB MK II), with an MgK_α X-ray source, operating at a vacuum of 10^{-8}–10^{-6} torr. Survey and high-resolution spectra of the phosphate layers at the surface and at different strata of the coatings were obtained using the argon-ion sputtering technique. Qualitative and quantitative information regarding each layer of the phosphate coatings was obtained from the precise determination of binding energies and integrated peak areas on the intensity versus binding energy plots obtained using a dedicated Apple II computer, interfaced with the spectrometer.

Phosphated test specimens of $1\ cm^2$ area where anodically polarized using an Elico (CL-95 model potentiostat, in a potential range of -0.8 to $+0.4$ V at a scan rate of $1.2\ V\,h^{-1}$, following a 15 min prepolarization immersion. A solution of 0.6 M ammonium nitrate was used as the electrolyte and potential measurements were made against the saturated calomel reference electrode and a platinum counter electrode. A plot of potential versus current density was recorded.

The phosphated samples from the reference bath and the baths containing 1-ODol and 1-ODT were subjected to the salt spray test (ASTM B-117-87) for 960 h after which they were assessed for the extent of lateral rust-creep from the scribed region.

3. Results and discussion

The coatings obtained in the reference bath and bath containing 1-ODol were greyish-white and adherent. However, the coatings obtained in the presence of 1-ODT showed the presence of scattered reddish-brown spots on them (Table I). As mentioned in our earlier studies [21], these reddish-brown spots dissolved completely in carbon tetrachloride and were identified (by chemical analysis and infrared spectroscopy) to be octadecylthionitrite, a reaction product of the added thiol with nitrous acid generated *in situ* in the phosphating bath during processing. Although the panels phosphated in the presence of 1-ODol and 1-ODT had significantly lower coating weight as

TABLE I Properties of the formulated baths

Bath used	Additive used	Structure of the additive	Optimum conc. ($mg\,l^{-1}$)	Appearance of the coating	Average[a] coating weight ($g\,m^{-2}$)
I (Reference bath)	–	–	–	Greyish-white, uniform, adherent	9.26
II	1-Octadecanol (1-ODol)	$C_{18}H_{37}OH$	50	Greyish-white, uniform, adherent	6.74
III	1-Octadecane thiol (1-ODT)	$C_{18}H_{37}SH$	75	Greyish-white, Scattered reddish-brown spots, adherent	6.72

[a] Average of five determinations.

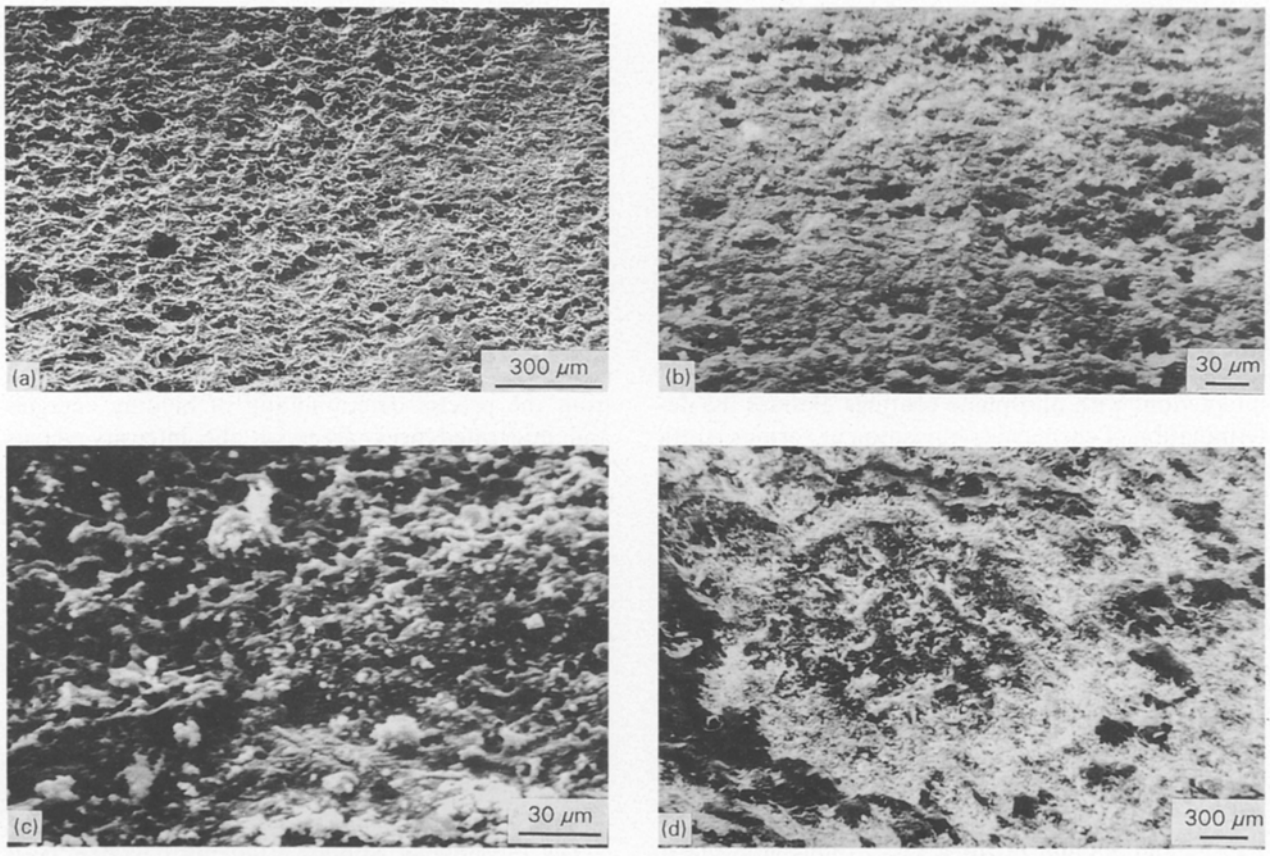

Figure 1 Scanning electron micrographs of coatings obtained from the reference bath after (a) 1 min (b) 30 min, and for coatings obtained after phosphating for 30 min in the presence of (c) 1-ODol and (d) 1-ODT.

compared to those coated in the reference bath (Table I), they showed lower porosity [22]. The decrease in coating weight in baths containing these additives was envisaged to be the result of their incorporation into the coatings through an adsorption mechanism. In order to gain insight into the details of structure and composition of these coatings, instrumental methods of evaluation were used.

3.1. Surface morphology

The surface microtopography of panels coated in the reference bath for a period of 30 min is shown in Fig. 1b. It is clear from the photomicrographs that coatings obtained from this bath were thick, dense and uniform. In order to investigate the nature and distribution of nuclei of crystals in the earlier stages of the phosphating process, the scanning electron micrographs of panels phosphated for a period of 1 min were obtained (Fig. 1a). It is observed that a uniform thin layer of coating deposition had already occurred; however, the coating showed considerable porosity.

The photomicrographs obtained after phosphating the panels for 30 min in baths containing 1-ODol and 1-ODT are shown in Fig. 1c and d, respectively. While panels coated in the presence of 1-ODT were characterized by dense, fine-grained coatings of low porosity, nodular congregations of fine crystallites were present on panels coated in the presence of 1-ODol. The latter coatings also showed higher porosity. The red spotted regions on panels coated in the presence of 1-ODT (as indicated by the dark central portions in Fig. 1d) showed no distinct morphological features. However, coating thickness was lower in these regions as compared to the surrounding fine-crystalline regions.

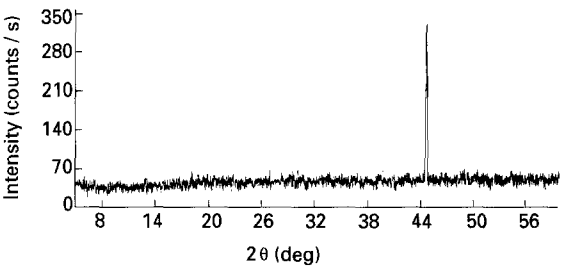

Figure 2 X-ray diffractogram of steel panel coated in the reference bath.

3.2. X-ray diffraction

Fig. 2 shows the X-ray diffractogram obtained for the steel panel coated in the reference bath. Except for the major peak at a 2θ angle of 44.6° which corresponds to that of α-iron of the substrate metal [15], no significant peaks characteristic of hopeite, phosphophyllite or scholzite were present. The absence of peaks corresponding to these typical phosphate phases in the coating may be attributed to the very fine-grained nature of the coating which lends it a near-amorphous nature [23, 24]. It is further interpreted to be the result of addition of a grain-refining agent, namely, calcium, in the phosphating composition [25]. Another associated cause for the microcrystallinity reflected in the

X-ray diffraction pattern obtained in this case is that the coatings were produced at room temperature, unlike traditional crystalline phosphate coatings which are produced from high-temperature baths. Diffraction patterns identical to that of coatings from the reference bath were also obtained in the cases of panels phosphated in the additive-containing baths. The absence of typical grain-like nuclei in the early stages of phosphating [1, 2, 26] in the scanning electron micrographs of panels coated for 1 min in the reference bath (Fig. 1a) support the above structural information obtained from the X-ray diffraction study.

3.3. X-ray photoelectron spectroscopy

Fig. 3 represents the survey spectra obtained at the unetched surfaces of phosphate coatings formed using the reference bath and the additive-containing baths. The survey spectrum of the uncoated steel surface is included for effective comparison. Carbon, oxygen, phosphorus, iron and zinc were detected on the surface of samples coated in the reference and 1-ODol-containing baths. Additional peaks corresponding to sulphur were observed in the spectra of coatings obtained in the presence of 1-ODT.

The significant increase in the intensity of the carbon peak in the panels coated in each of the additive-containing baths, and the detection of sulphur on the unetched surfaces of samples coated in the presence of 1-ODT indicated the incorporation of these additives into the phosphate coatings obtained from these baths. Further, it evinced the ability of these surfactants to form films on the coated surface. The effectiveness of these additive films in sealing the pores of the phosphate coatings is evident from the observation that the XPS signature peaks of iron (at binding energy values of 708 and 721 eV) were diminished or had disappeared in panels coated using the additive-containing baths, despite the fact that coating weight obtained in the presence of these additives was significantly (27%) less than that of the reference bath.

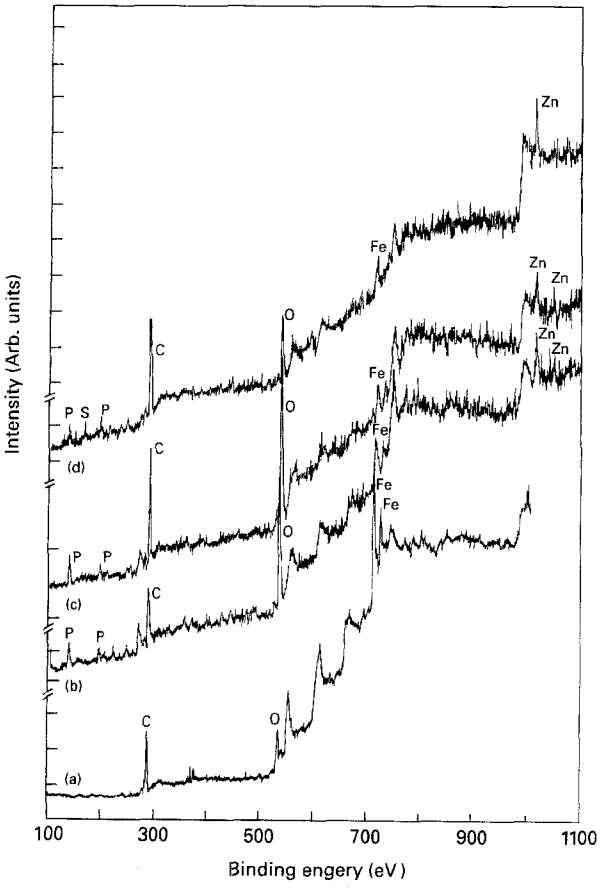

Figure 3 Survey spectra of (a) uncoated steel, and phosphate coatings obtained in (b) the reference bath, (c) 1-ODol-containing bath, and (d) 1-ODT-containing bath.

In order to ascertain whether the influence of these additives was restricted to the formation of surface films, or whether these surfactants participated at every stage of coating formation, depth-profiling studies were carried out. Fig. 4a–d show the concentration profiles of the constituent elements of the coatings obtained in the reference and additive-containing baths, as a function of sputter time. The following trends were observed in the elemental concentrations in the formulated baths.

3.3.1. Bath containing 1-ODol

The surface of specimens coated in the presence of 1-ODol were rich in carbon and oxygen (Fig. 4b). The carbon content decreased significantly with sputtering, being the lowest at a sputter time of 10 min. However, on increasing the sputter time to 40 min, the carbon content increased. This evinced the fact that layers close to the metal substrate were richer in carbon than the intermediate layers. This may be correlated to the adsorption of the aliphatic long-chain additives at the surface of the metal during the initial stages of coating deposition. High-resolution spectra obtained at each stage of sputtering indicated that the carbon peak appeared at 286.25 eV, which correlated well with the binding energy of the C–O bond [27]. This suggested that the alcohol was present at every stage of coating formation. This conclusion is further supported by the observation that at all strata of the coating, the carbon content in panels coated in the presence of 1-ODol was considerably higher than that of the reference bath (Fig. 4a).

The variations in the relative percentage of iron with sputter time showed that the iron content was lower in baths containing 1-ODol than the reference. It can also be seen that the intermediate layers of the coating were rich in phosphorous and zinc and that the concentrations of these elements diminished as the substrate was approached (sputter time of 40 min).

3.3.2. Bath containing 1-ODT

The surface layers of the unsputtered sample coated in the presence of 1-ODT was rich in carbon, oxygen and sulphur, while it contained relatively low concentrations of zinc and iron (Fig. 4c). After sputtering for 5 min, there was a significant decrease in the carbon content in the coating. Also, it was observed that there was a remarkable increase in the concentration of phosphorus, after the carbon-rich surface layer was

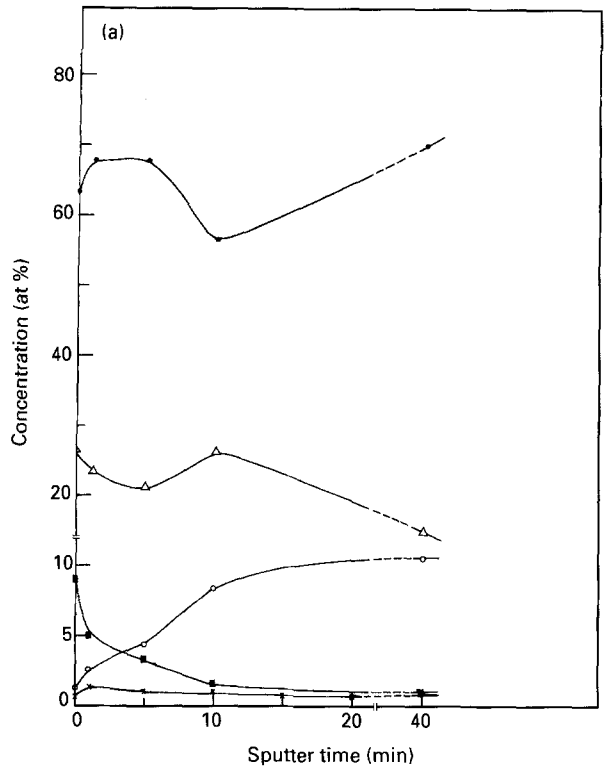

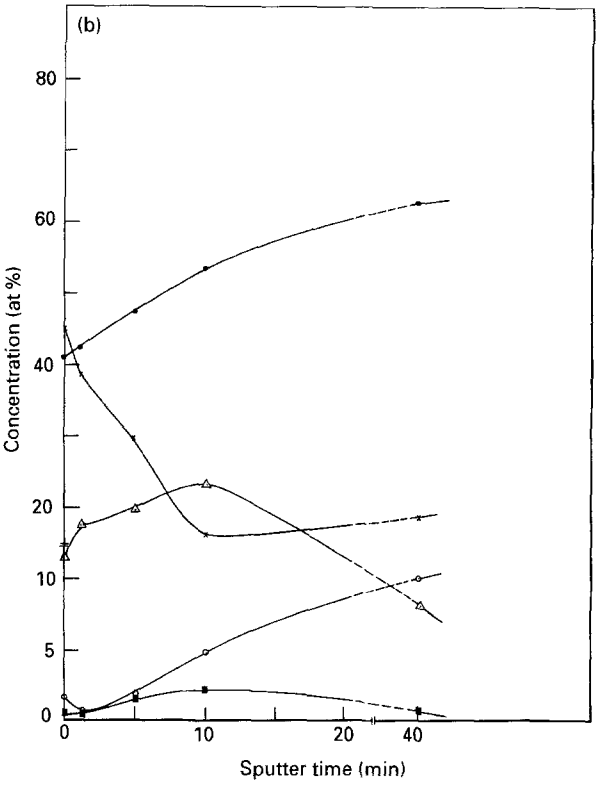

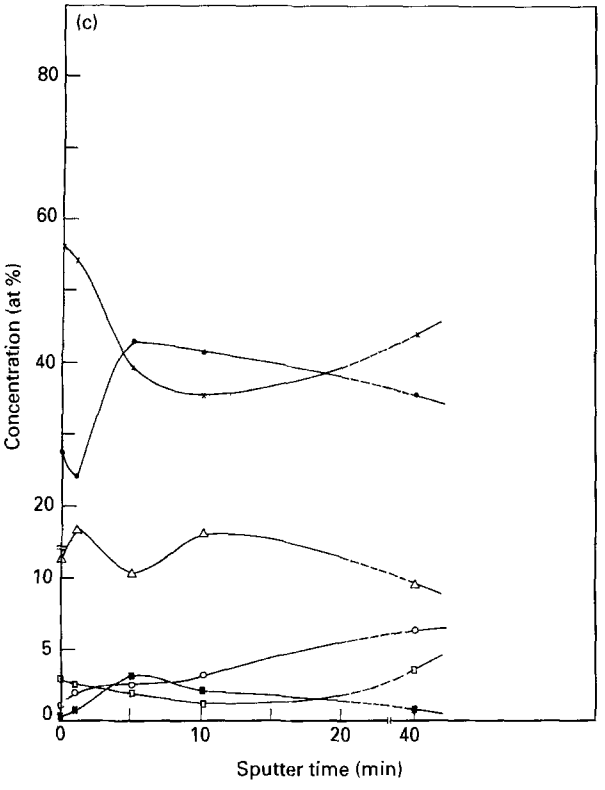

Figure 4 Elemental concentration profiles of phosphate coatings obtained using the (a) reference bath, (b) bath containing 1-ODol, (c) bath containing 1-ODT. (●) Oxygen, (▲) phosphorus, (○) iron, (×) carbon, (■) zinc, (□) sulphur.

removed by sputtering for 1 min. However, the phosphorus content decreased sharply as the substrate was approached (sputter time of 40 min). It is also evident that the layers closest to the metal substrate were rich in carbon, sulphur and iron though they were depleted of zinc.

The trends observed in the changes in the concentrations of the constituent elements of the coating at different depths support the mechanism suggested earlier [21] to explain the action of 1-ODT in the formulated bath. The high concentrations of alkyl carbons (binding energy of 284.8 eV) close to the substrate, as compared to the intermediate layers, evinced the adsorption of 1-ODT on the panel being phosphated. It may be considered that the adsorbed additive existed mainly as the thiol (in the underivatized form) when adsorption occurred, as the high-resolution spectrum of sulphur, at the layer close to the substrate showed a peak at 162.25 eV, which correlated well with that of 1-ODT [28]. The *in situ* derivatization of $C_{18}H_{37}SH$ into the thionitrite, though visually observed and analytically confirmed, could not be evinced from the XPS studies, probably due to the low concentration of the derivative formed. However, the evident incorporation of sulphur into the growing layers of the phosphate coating indicate that coating deposition was regulated at every stage by thiol adsorption.

The XPS studies provide conclusive evidence of the integration of additives not only at the metal surface but also at all stages of coating deposition. The increased concentration of carbon at the surface layers of coatings obtained in the presence of these additives indicate their ability to form surface films which would not only help in effectively sealing the pores of the coating but also prevent moisture ingress due to their hydrophobic nature. The incorporation of the additives into the growing layers of the phosphate coating substantiates the observations made in the SEM study that fine-grained coatings are obtained. The additives, through their adsorption at various stages of coating deposition, favour the controlled growth of crystals which result in well-packed and compact coatings.

The combined effects of fine-grained, compact coatings of low porosity and their considerable hydrophobicity, lead to the expectation that coatings obtained in the formulated baths would show satisfactory performance in corrosive environments. The relative efficiencies of the additives as well as their performance in comparison with samples coated in the reference bath, were evaluated using the electrochemical anodic polarization method and the salt spray test.

Fig. 5 represents the anodic polarization curves obtained for the panels coated in the reference and additive-containing baths. The polarization curve obtained for uncoated steel has been included for effective comparison.

As reported earlier [29], the appearance of two current density maxima is unique to phosphated samples and the second current density maximum (around 0.00 mV) has been ascribed to be due to the dissolution of the phosphate coating followed by competitive and potential-dependent adsorption of anions at the steel surface during anodic polarization.

The magnitude of current density at the first current maximum (around − 0.40 mV), can be related to the ohmic resistance of the phosphate coating which, in turn, is related to coating quality [30]. It can thus be inferred that the coatings obtained in the presence of these long-chain additives were of good quality, as they showed high ohmic resistance (lesser current flow). The proximity of values of current density obtained for these additives having similar long alkyl carbon chains, but different functional groups, suggested that chain length governed this parameter rather than additive functionality.

Beyond the first current maximum, the anodic dissolution process is hindered by the adsorption of hydroxy ions which passivate the substrate. This results in a decrease in current density. Further polarization up to the second current maximum causes an increase in current flow due to acceleration of steel corrosion in this range by the dissolved phosphate ions which displace the passivating hydroxyl ions [29]. Table II shows the values of current density obtained at the second current maximum in the case of the additive-containing as well as the reference baths. Because the availability of phosphate ions (through their dissolution from the coating during anodic polarization) is decisive in determining the magnitude of the second

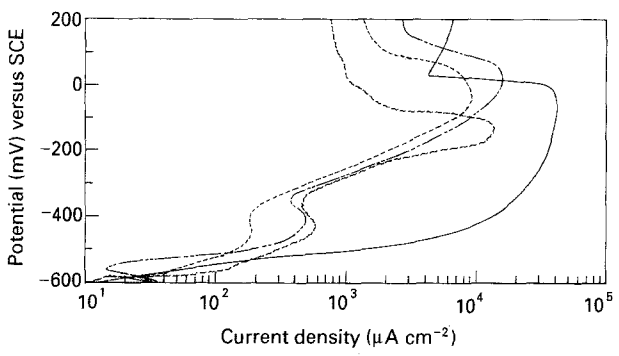

Figure 5 Anodic polarization curves of the phosphate coatings obtained in the reference and additive-containing baths: (——) uncoated, (– – –) reference, (— — — —) ODol, (~ ~ ~) ODT.

TABLE II Corrosion performance

Sample used	Current density at 2nd current maximum (mA cm^{-2})	Observation after salt spray test
Uncoated	42.10	Considerable lateral rust-creep from scribe
Phosphated in the reference bath	9.22	Minimal rust-creep from scribe
Phosphated in presence of 1-ODol	15.33	Minimal rust-creep from scribe
Phosphated in presence of 1-ODT	13.34	Minimal rust-creep from scribe

current maximum, the decreased current density values obtained for coatings formed in the presence of the long-chain thiol indicates their better quality as compared to those coated in the presence of the long-chain alcohol. The comparably low current densities of the second current maximum obtained from the additive-containing baths as compared to the reference bath may be correlated to the decreased porosity and compact nature of the coatings obtained from these baths.

The results obtained from the anodic polarization studies were supported by the results of the salt spray test. Despite the substantial decrease in the coating weight of samples phosphated in the additive-containing baths as compared to the reference bath, the extent of rust-creep after 960 h salt spray was similar in both the cases (Table II). This can be related to the low moisture uptake and permeability of these coatings, resulting from the integration of the hydrophobic hydrocarbon chains of these long-chain compounds, thus retarding the onset of corrosion that may arise out of any moisture ingress through the organic topcoat. Further, the fine-grained nature of the coatings affords excellent interaction between the topcoat and the phosphate pretreatment, thereby minimizing the effects of corrosion-induced de-adhesion when subjected to aggressive environments.

4. Conclusion

Phosphate coatings obtained from cold zinc phosphating baths containing 18-carbon alcohol and thiol additives were characterized. It was observed that the coatings obtained from the reference and additive-containing baths were uniform and adherent. The surface microtopography of these coatings studies using SEM indicated that the coatings obtained both in the presence and absence of these additives were fine-grained, resulting in the formation of dense, compact and uniform coatings. Further investigation into the nature of these coatings by X-ray diffraction technique indicated they were microcrystalline. XPS studies indicated that the additives not only controlled the extent of coating formation (through their adsorption) during the initial stages of coating deposition (nucleation) but also participated at every stage of coating

deposition (coating growth). These studies also provide conclusive evidence to substantiate the ability of these surface-active agents to form surface films on the phosphate coating, which would supplement the protection provided by the phosphate layer. Although the gross effect observed in the additive-containing baths was a decrease in coating weight, there was no compromise in their performance in corrosive environments. The major factors which contributed to their excellent corrosion performance are the ability of these additives to form protective, hydrophobic films which significantly reduce moisture ingress and stifle the initiation and propagation of corrosion.

Acknowledgements

The authors thank the Regional Sophisticated Instrumentation Centre and the Materials Science Research Centre, Indian Institute of Technology, Madras, India, for providing the facilities to carry out SEM, XPS and XRD studies. The financial support extended by the Council of Scientific and Industrial Research (CSIR), New Delhi, India, is also gratefully acknowledged.

References

1. G. LORIN, "Phosphating of Metals" (Finishing publications, London, 1974) p. 158.
2. D. B. FREEMAN, "Phosphating and Metal Pretreatment" (Woodhead–Faulkner, London, 1986) p. 51.
3. E. L. GHALI and R. J. A. POTVIN, *Corros. Sci.* **12** (1972) 583.
4. K. KISS and M. COLL-PALAGOS, *Corrosion* **43** (1987) 8.
5. R. W. ZURILLA and V. HOSPADARUK, *Trans. SAE* 780187 **87** (1978) 762.
6. J. P. SERVAIS, B. SCHMITZ and V. LEROY, *Mater. Perform.* **27** (1988) 56.
7. D. D. DAVIDSON, M. L. STEPHENS, L. E. SOREIDE and R. J. SHAFFER, *Trans. SAE* 862006 **95** (1986) 1045.
8. T. SUGAMA, L. E. KUKACKA, N. CARCIELLO and J. B. WARREN, *J. Appl. Polym. Sci.* **30** (1985) 2137.
9. N. SATO, T. MINAMI and H. KONO, *Surf. Coat. Technol.* **37** (1989) 23.
10. G. RUDOLPH and H. HANSEN, *Trans. Inst. Met. Finish.* **50** (1972) 33.
11. K. NOMURA and Y. UJIHIRA, *J. Mater. Sci.* **17** (1982) 3437.
12. N. SATO, K. WATANABE and T. MINAMI, *ibid.* **26** (1991) 1383.
13. N. SATO and T. MINAMI, *ibid.* **24** (1989) 4419.
14. A. NEUHAUS and M. GEBHARDT, in "Interface Conversion for Polymer Coatings", edited by P. Weiss and G. D. Cheever (American Elsevier, New York, 1968).
15. M. O. W. RICHARDSON and D. B. FREEMAN, *Trans. Inst. Met. Finish.* **64** (1986) 16.
16. N. S. McINTYRE, in "Applied Electron Spectroscopy for Chemical Analysis", edited by H. Windawi and F. F. L. Ho, Vol. 63, Chemical Analysis Monograph Series (Wiley, New York, 1982) p. 89.
17. W. J. VAN OOIJ, in "Organic Coatings: Science and Technology", edited by G. D. Parfitt and A. V. Patsis, Vol. 6 (Marcel Dekker, New York, 1984) p. 277.
18. L. FEDRIZZI and F. MARCHETTI, *J. Mater. Sci.* **26** (1991) 1931.
19. T. SUGAMA, L. E. KUKACKA, N. CARCIELLO and J. B. WARREN, *J. Appl. Polym. Sci.* **30** (1985) 4357.
20. N. SATO, *J. Metal. Finish. Soc. Jpn* **38** (1987) 30.
21. U. B. NAIR and M. SUBBAIYAN, *Metal Finish.* **91** (1993) 17.
22. *Idem, Trans. Inst. Met. Finish.* in press.
23. A. DOUTY, E. STOCKBOWER and W. C. JONES, in "Electroplating Engineering Handbook", 4th Edn, edited by L. J. Durney (Van Nostrand Reinhold, New York, 1984).
24. S. C. TUNG, D. J. SMOLENSKI and S. S. WANG, in "Proceedings of the 17th Conference on Metallurgical Coatings", and "8th International Conference on Thin Films", San Diego, April 1990.
25. G. N. BHAR, N. C. DEBNATH and S. ROY, *Surf. Coat. Technol.* **35** (1988) 171.
26. H. W. K. ONG, L. M. GAN and T. L. TAN, *J. Adhes.* **20** (1986) 117.
27. S. H. HERCULES and D. M. HERCULES, *Rec. Chem. Progr.* **32** (1971) 183.
28. R. V. DUEVEL and R. M. CORN, *Anal. Chem.* **64** (1992) 337.
29. R. L. CHANCE and W. D. FRANCE Jr, *Corrosion* **8** (1969) 329.
30. R. A. MACHEVSKAYA, L. D. MURIENKO and N. A. BABAKINA, *Prot. Met.* **11** (1975) 198.

Received 23 August 1993
and accepted 27 July 1994